

UCSF

UC San Francisco Previously Published Works

Title

CDKN2B Regulates TGF β Signaling and Smooth Muscle Cell Investment of Hypoxic Neovessels.

Permalink

<https://escholarship.org/uc/item/9rq6g7w6>

Journal

Circulation research, 118(2)

ISSN

0009-7330

Authors

Nanda, Vivek
Downing, Kelly P
Ye, Jianqin
[et al.](#)

Publication Date

2016

DOI

10.1161/circresaha.115.307906

Peer reviewed



Published in final edited form as:

Circ Res. 2016 January 22; 118(2): 230–240. doi:10.1161/CIRCRESAHA.115.307906.

***CDKN2B* Regulates *TGFβ* Signaling and Smooth Muscle Cell Investment of Hypoxic Neovessels**

Vivek Nanda¹, Kelly P. Downing¹, Jianqin Ye¹, Sophia Xiao¹, Yoko Kojima¹, Joshua M. Spin², Daniel DiRenzo¹, Kevin T. Nead¹, Andrew J Connolly³, Sonny Dandona⁴, Ljubica Perisic⁵, Ulf Hedin⁵, Lars Maegdefessel⁶, Jessie Dalman¹, Liang Guo⁷, XiaoQing Zhao⁷, Frank D. Kolodgie⁷, Renu Virmani⁷, Harry R. Davis Jr⁷, and Nicholas J. Leeper^{1,2}

¹Surgery, Stanford University School of Medicine, Stanford, California, USA

²Medicine, Stanford University School of Medicine, Stanford, California, USA

³Pathology, Stanford University School of Medicine, Stanford, California, USA

⁴Medicine, McGill University, Montreal, Canada

⁵Molecular Medicine and Surgery, Karolinska Institute, Stockholm, Sweden

⁶Medicine, Karolinska Institute, Stockholm, Sweden

⁷CVPath Institute, Gaithersburg, Maryland, USA

Abstract

Rationale—Genetic variation at the chromosome 9p21 cardiovascular risk locus has been associated with peripheral artery disease (PAD), but its mechanism remains unknown.

Objective—To determine whether this association is secondary to an increase in atherosclerosis, or is the result of a separate angiogenesis-related mechanism.

Methods and Results—Quantitative evaluation of human vascular samples revealed that carriers of the 9p21 risk allele possess a significantly higher burden of immature intraplaque microvessels than carriers of the ancestral allele, irrespective of lesion size or patient comorbidity. To determine whether aberrant angiogenesis also occurs under non-atherosclerotic conditions, we performed femoral artery ligation surgery in mice lacking the 9p21 candidate gene, *Cdkn2b*. These animals developed advanced hind-limb ischemia and digital auto-amputation, secondary to a defect in the capacity of the *Cdkn2b*-deficient smooth muscle cell (SMC) to support the developing neovessel. Microarray studies identified impaired *TGFβ* signaling in cultured *CDKN2B*-deficient cells, as well as *TGFβ1* upregulation in the vasculature of 9p21 risk allele carriers. Molecular signaling studies indicated that loss of *CDKN2B* impairs the expression of the inhibitory factor, *SMAD-7*, which promotes downstream *TGFβ* activation. Ultimately, this manifests in the upregulation of a poorly studied effector molecule, *TGFβ1-induced-1*, which is a

Address correspondence to: Dr. Nicholas J. Leeper, Divisions of Vascular Surgery and Cardiovascular Medicine, Stanford University, 300 Pasteur Drive, Room H3638, Stanford, California 94305, Tel: 650 724 8475, Fax: 650 498 6044, nleeper@stanford.edu.

DISCLOSURES

The authors have declared that no conflict of interest exists.

TGFβ ‘rheostat’ known to have antagonistic effects on the EC and SMC. Dual knockdown studies confirmed the reversibility of the proposed mechanism, in vitro.

Conclusions—These results suggest that loss of *CDKN2B* may not only promote cardiovascular disease through the development of atherosclerosis, but may also impair *TGFβ* signaling and hypoxic neovessel maturation.

Subject Terms

Atherosclerosis; Gene Expression and Regulation; Pathophysiology; Peripheral Vascular Disease; Risk Factors

Keywords

Atherosclerosis; peripheral artery disease; angiogenesis; cardiovascular disease *CDKN2B*; 9p21; *TGFβ*

INTRODUCTION

CDKN2B is a highly conserved cell-cycle regulator and tumor suppressor gene implicated in the pathogenesis of several malignancies¹. Recently, however, *CDKN2B* has also been implicated as a candidate gene which may be responsible for a portion of the genetic risk concentrated at the chromosome 9p21 cardiovascular genome-wide association study (GWAS) locus^{2, 3}. We previously reported that loss of *Cdkn2b* alters the blood vessel’s response to both mechanical injury⁴ and chronic atherosclerosis⁵, potentially providing insights into how the 9p21 locus potentiates both abdominal aortic aneurysm disease (AAA) and myocardial infarction (MI).

Interestingly, the 9p21 locus has now been associated with several other potentially non-overlapping vascular phenotypes, including non-atherosclerotic intracranial berry aneurysms and peripheral artery disease (PAD)^{6–9}. Amongst these, PAD is increasingly recognized as a growing public health concern, which now affects over 200 million individuals worldwide and accounts for every ~5th cardiovascular healthcare dollar spent^{10, 11}. PAD is interesting in that it shares several atherosclerosis-related risk factors with coronary artery disease (CAD), but also appears to be driven by a variety of PAD-specific mechanisms, including pathways related to angiogenesis and the response to hypoxia¹². Accordingly, the aim of this study was to determine the role of *Cdkn2b* in a non-atherosclerotic ischemic injury model, with the goal of advancing our understanding of how the 9p21 locus simultaneously promotes an individual’s heritable risk for so many divergent clinical phenotypes.

METHODS

Detailed methods are available in the Online Data Supplement.

Human studies

Coronary arteries were dissected from the hearts of victims of sudden cardiac death, paraffin-embedded, serially sectioned at 3- to 4-mm intervals, processed for histological

examination, and visualized at the CVPath Institute (Gaithersburg, Maryland), as previously described¹³. Microvessel density (MVD) was computed as the total number of CD31⁺CD34⁺ vessels/total area, and mural cell coverage as α SMA⁺ microvessel/total microvessel (Ulex⁺). Genotyping for rs1333049 was performed using TaqMan SNP allelic discrimination genotyping assay (Cat. # 4351379, Life Technologies) on an Applied Biosystems 7500 Fast Real-Time PCR System following DNA extraction from sections using Genra Puregene Tissue Kit or QIAamp DNA FFPE Tissue Kit (Qiagen) according to the manufacturer's instruction. All histomorphometric quantification were performed in a blinded fashion and locked into a database prior to performing genotyping and data analysis. Collection, storage, and use of tissue and patient data were performed in agreement with institutional ethical guidelines.

In an independent study designed to correlate genotype with gene expression, DNA and RNA were extracted from vascular specimens harvested from patients undergoing surgery for carotid stenosis, as part of the Biobank of Karolinska Endarterectomy (BiKE) study. Samples were analyzed by Affymetrix HG-U133 plus 2.0 microarrays and Illumina 610w - QuadBead SNP-chips, as previously described^{5, 14}, and deposited in Gene Expression Omnibus (accession number GSE21545). Pearson's correlations were calculated to determine association between expression of gene of interest and other genes from microarrays.

Murine studies

Wild type and *Cdkn2b*^{-/-} mice on a C57Bl/6 background were subjected to femoral artery ligation to induce hindlimb ischemia, as previously described. Subsequent immunohistochemistry, gene expression, vessel density, vascular permeability and ambulatory impairment studies were performed, as described in the Supplemental materials^{15, 16}. All studies were approved by the Stanford University Administrative Panel on Laboratory Animal Care.

Cell culture

Commercially available human coronary artery SMCs (HCASMCs, hereafter referred to as SMCs) and human umbilical vein ECs (HUVECs, hereafter referred to as ECs) were purchased from Lonza and cultured in growth medium according to the manufacturer's (Lonza) instructions. In order to simulate hypoxic conditions, cultured cells were incubated in a sealed chamber filled with 2% oxygen for at least 6h following which mRNA or protein was isolated. Knockdown and overexpression studies were performed by transfecting cells with Lipofectamine RNAiMAX (Life Technologies) and Lipofectamine 3000 (Life Technologies) respectively, as per the manufacturer's instructions.

***In vitro* studies**

Gene expression was determined using Applied Biosystem's ViiATM7 RT-PCR system. Data generated was normalized to 18S as previously described¹⁷ and expressed as a fold-change in in gene expression. Experimental details for the Boyden chamber cell migration, EC permeability, cell viability, Western blot, ELISA and angiogenesis assays are provided in the Supplemental materials^{4, 18}. Tube formation was studied by plating transfected ECs in μ

slides (ibidi) precoated with Matrigel (BD Biosciences), exposed to conditions simulating hypoxia or normoxia for 24 h, then photographed using a phase contrast inverted microscope (Nikon), prior to a blinded quantification of new tubes formed. In certain experiments, the co-localization of co-cultured ECs and SMCs was assessed using Adobe PhotoshopCS5.1.

Microarray assays

RNA samples from primary cell cultures were verified by Agilent 2100 Bioanalyzer, pooled by treatment group, and labeled and hybridized to the Human HT-12v4 Beadchip Platform (Illumina). Arrays (n = 4 per condition) were scanned using a Microarray Scanner and Feature Extractor (software v 9.5.1) and analyzed with Genespring GX 13.0.2 (Agilent). Confirmatory pairwise analysis was performed between conditions using Statistical Analysis of Microarrays (SAM v 4.0) with false detection ratio (FDR) < 1¹⁹. Genes which were consistently dysregulated in both ECs and SMCs were then subjected to bioinformatics analyses. Enrichment for KEGG (Kyoto Encyclopedia of Genes and Genomes) pathway categories and GO (Gene Ontology) biological process categories were determined using DAVID Bioinformatics Resources 6.7 (NCBI), with p < 0.05 EASE cutoff²⁰. All microarray data were submitted to the National Center for Biotechnology Information's Gene Expression Omnibus.

Statistical analysis

Data are presented as mean ± standard error using GraphPad Prism 6. In experiments where two groups were compared, analysis was performed with unpaired two-tailed T-testing assuming Gaussian distribution. In experiments with more than two groups, analysis was performed with ANOVA and post-testing performed using the method of Tukey. Differences were deemed significant when the *P* value was found to be less than 0.05. Data from each experiment was replicated at least three times and all analyses were performed in a blinded fashion. All microarray studies employed Student's T-tests with correction for multiple comparisons according to the Sidak-Bonferroni method with correlations determined by Pearson's analysis. In all figures: + < 0.05, # < 0.01, ** < 0.001.

RESULTS

Carriers of the 9p21 cardiovascular risk allele display pathological angiogenesis and impaired vessel maturation within their atherosclerotic lesions

Amongst the 66 individuals genotyped in the autopsy cohort, 12 were found to be homozygous for the 9p21 risk allele rs1333049 (C/C), 24 had only the ancestral allele (G/G), and 29 were heterozygous (C/G). Importantly, the 9p21 genotype was not associated with any recorded clinical variable, including age, gender, BMI, or cardiovascular risk factors such as smoking, hypertension, diabetes or dyslipidemia (*P* > 0.21 for each phenotype measured, Supplemental Table IA). A total of 88 coronary arteries were analyzed (14 from C/C, 36 from G/G, 38 from C/G), and intraplaque CD31⁺CD34⁺ microvessel density was found to be significantly higher in the carriers of the risk allele than in those with the ancestral allele (*P* for trend across genotype < 0.05, Figure 1A). This trend occurred across the spectrum of lesion phenotypes and irrespective of plaque size (Supplemental

Figure I). Next, mural cell coverage of these microvessels was quantified by measuring the presence of α -SMA-positive smooth muscle cells surrounding the Ulex-positive endothelial tubes, as previously described¹³. This analysis revealed that intraplaque vessels present in lesions obtained from carriers of the risk allele were significantly less likely to be enveloped by adjacent SMCs, relative to those from carriers of the ancestral allele (P for trend across genotype < 0.05 , Figure 1B), even after controlling for comorbidities (Supplemental Table IB). Together, these findings suggest that the 9p21 risk allele may promote neovessel formation, but impair microvessel maturation within the atherosclerotic plaque.

Loss of the 9p21 candidate gene, *Cdkn2b*, promotes critical limb ischemia and impairs ischemic vessel maturation, in vivo

To determine whether the microvascular phenotype observed above is restricted to the atherosclerotic plaque or if it may also occur under non-atherosclerotic conditions, we next subjected mice deficient in the 9p21 candidate gene, *Cdkn2b*, to femoral artery ligation surgeries. Importantly, *Cdkn2b*^{-/-} mice did not display a baseline defect in vascular anatomy, as quantified by absolute EC content (CD31 staining), SMC content (α -SMA staining), and capillary density (CD31⁺ vessels/mm fiber) in unligated, non-ischemic limbs, relative to *Cdkn2b*^{+/+} mice ($P > 0.53$ for all assays, Supplemental Figure IIA). Fourteen days after inducing hindlimb ischemia in this non-atherosclerotic model, however, *Cdkn2b*^{-/-} mice developed significantly worse critical limb ischemia (2.7 vs. 3.9 mean clinical tissue damage units, $P < 0.05$, Figure 2A) and ambulatory impairment scores (1.7 vs. 2.4 mean ambulatory impairment units, $P < 0.05$, Figure 2B) than wild type animals, as assessed by a blinded scorer. Laser Doppler imaging confirmed that this phenotype was secondary to a perfusion defect in *Cdkn2b*^{-/-} mice, relative to *Cdkn2b*^{+/+} mice ($P < 0.0001$ via two way ANOVA, Figure 2C–D). Representative images revealed that these animals sustained substantial tissue loss and digital autoamputation, indicative of advanced ischemia (Figure 2E). Quantitative histologic analysis revealed that the ischemic hindlimbs of *Cdkn2b*^{-/-} mice contained reduced vascular density (as assessed by the number of CD31⁺ vessels/mm fiber, Supplemental Figure IIB) and that there was a significantly higher burden of immature neovessels not invested by mature SMCs (as quantified by the ratio of α -SMA-to-CD31 content in the ischemic hindlimb; 0.12 vs 0.57, $P < 0.01$, Figure 2F). TUNEL staining failed to identify a difference in vascular apoptosis across genotypes in the hypoxic limbs (data not shown), but Evan's Blue analyses revealed a trend towards increased vascular permeability in the ischemic hindlimbs of *Cdkn2b*^{-/-} mice (Supplemental Figure IIC). Qualitative microCT scans suggest that *Cdkn2b*^{-/-} have lower vascular density than wild type mice, after an ischemic insult (Supplemental Figure IID).

Loss of CDKN2B promotes angiogenic behavior in endothelial cells, but impairs smooth muscle cell recruitment to developing vessels, in vitro

After confirming efficient knockdown (Supplemental Figure IIIA–B), we next performed a series of in vitro assays to understand how loss of *Cdkn2b* could impair vessel maturation under hypoxic conditions. We found that hypoxic *CDKN2B*-deficient (si*CDKN2B*) ECs displayed several pro-angiogenic features relative to control transfected (si*Cont*) cells, including: 1. Enhanced migration in a scratch test assay (71.7% vs 43.1% wound healing, $P < 0.001$, Figure 3A); 2. Increased proliferation in an MTT assay (1.51 vs 1.01 relative

proliferation units, $P < 0.001$, Figure 3B); 3. Greater expression of the angiogenic cytokine *VEGF* (6.9 vs 2.3 fold increase relative to baseline, $P < 0.001$, Figure 3C); 4. Increased tube formation in a Matrigel assay (1.07 vs 0.82 tubes/hpf, $P < 0.001$, Figure 3D); and 5. Increased endothelial permeability in a barrier diffusion assay (54.7% increase, $P < 0.001$, Supplemental Figure IIIC). Conversely, while we found that *CDKN2B*-deficient SMCs displayed significantly greater migration than control-transfected SMCs at baseline (58.8% increase, $P < 0.001$), we found that this effect on chemokinesis was lost under hypoxic conditions (10.2% increase, $P = \text{NS}$, Figure 3E). In an attempt to model vessel maturation in vitro, we then co-cultured *CDKN2B*-deficient ECs and SMCs together in Matrigel, and quantified tube formation and investment by mural cells. In keeping with the findings provided above (Figure 1B and 2F), we found that hypoxic *CDKN2B*-deficient neovessels were thin-walled and less likely to be supported by SMCs than control vessels (3.13 vs. 5.35, $P < 0.01$, Figure 3F).

Microarray studies implicate impaired TGF β signaling in *CDKN2B*-deficient vascular cells

To pursue the molecular mechanism by which loss of *CDKN2B* leads to the observed angiogenic defect, we next performed a series of cDNA microarray assays in *CDKN2B*-deficient ECs and SMCs. While each set of arrays identified a varying number of differentially regulated genes (Supplemental Table II), we found a collection of 247 genes which were consistently and significantly dysregulated in all *CDKN2B*-deficient cells, relative to control-transfected cells (Figure 4A). Bioinformatic analyses performed on this common list of genes revealed that 5 of the 8 conditions predicted to be associated with loss of *CDKN2B* by the Genetic Association Database for Disease Associations are phenotypes previously associated with the 9p21 risk locus through GWAS (Figure 4B, red)^{6, 21}. KEGG Pathway analysis identified “Angiogenesis” as the most significantly altered pathway in *CDKN2B*-deficient cells. Moreover, Panther and Gene Ontology (GO) analysis revealed that 12 of the 18 significantly enriched biological process terms associated with loss of *CDKN2B* involve angiogenesis-related processes (Figure 4B, brown) or specifically include dysregulation of a *TGF β* -family signaling member (Figure 4B, blue), implicating this latter pathway in the observed phenotype.

eQTL studies confirm anti-correlation of *CDKN2B* and TGF β 1 in human vascular tissue

To determine whether *TGF β* 1 signaling is also perturbed in the vasculature of subjects with reduced *CDKN2B* expression, we next evaluated 127 carotid endarterectomy samples from the BiKE Biobank. Carriers of the representative 9p21 risk allele (‘G’ at rs1412829, who we previously showed have significantly reduced vascular *CDKN2B* expression⁵), had a trend towards increased *TGF β* 1 expression within their atherosclerotic plaque (P for trend = 0.07, Figure 4C). Co-expression analysis revealed that *TGF β* 1 and *CDKN2B* expression were inversely correlated ($r^2 = -.4972$, $P < 0.0001$, Figure 4D), suggesting upregulation of *TGF β* 1 under conditions of reduced *CDKN2B* expression in the vessel wall.

Molecular signaling studies confirm that loss of *CDKN2B* promotes *TGF β* -auto-induction and upregulation of *TGF β 1i1*

Given the data presented above, we performed confirmatory ELISA assays, and found that hypoxic *CDKN2B*-deficient ECs and SMCs both secreted more *TGF β 1* than control transfected cells ($P < 0.01$ for each, Figure 4E). While a number of downstream *TGF β* -signaling family members were dysregulated in each of the EC and SMC microarrays performed above, the only factor which was consistently dysregulated (fold change > 1.5 , FDR < 1 by SAM) in each condition tested was a poorly-studied effector molecule known as *TGF β 1-induced-1* (*TGF β 1i1*). RT-PCR assays confirmed these microarray findings, and revealed that knockdown of *CDKN2B* led to a significant increase in the expression of *TGF β 1i1* in both hypoxic ECs and SMCs ($P < 0.05$ for each, Figure 4F). Subsequent Western blots directed at uncovering the mechanism by which loss of *CDKN2B* leads to the induction of *TGF β 1i1* revealed that knockdown of *CDKN2B* in hypoxic cells results in: 1. Downregulation of the key inhibitory factor, *SMAD7*; 2. Upregulation of *TGF β 1*; 3. Increased downstream *SMAD3* activation; and 4. An ultimate increase in *TGF β 1i1* (Figure 4G–H). In vitro, the changes in *SMAD7* and *TGF β 1* appear to occur at the post-transcriptional level, as no differences were observed in the mRNA levels of these genes across conditions (data not shown).

Dual knockdown studies suggest that the *CDKN2B*-dependent vascular maturation defect is reversible

To investigate the reversibility of the observed phenomenon, and prove that *TGF β 1i1* was the effector molecule responsible for the vascular maturation phenotype, we performed individual and simultaneous knockdown of *CDKN2B* and *TGF β 1i1* in cultured ECs and SMCs. As shown in Figure 5A, *CDKN2B* and *TGF β 1i1* individually had opposing effects in the Matrigel co-culture assay (top two panels, $P < 0.05$ for each); however, simultaneous inhibition of both factors led to a normalization in tube formation and vessel maturation, as quantified by SMC to EC ratio ($P = 0.92$, Figure 5A). Together, these data suggest that the hypoxic *CDKN2B*-dependent angiogenic defect could be reversed, at least in vitro. Similar effects were observed in cells overexpressing *SMAD7* (Supplemental Figure IIID–E), further supporting the molecular pathway proposed in Figure 5B.

DISCUSSION

The studies presented above suggest that carriers of the 9p21 risk allele, whom we have previously shown to have reduced vascular expression of *CDKN2B*⁵, experience an imbalance in endothelial tube formation and neovessel maturation in the vessel wall. We find that this defect is not restricted to atherosclerotic conditions, and show that loss of *Cdkn2b* impairs the ability of the SMC to support neovessel development and tissue perfusion in a non-atherosclerotic animal model of PAD. Molecular studies suggest that these defects are the result of a previously unappreciated *TGF β* auto-induction cascade, which culminates in the upregulation of a complicated and poorly studied effector molecule, *TGF β 1i1*. Together, these findings provide a possible mechanism for how a top PAD GWAS locus modifies the risk for peripheral vascular disease⁷, and may do so

independently of its described effects on atherosclerosis⁶ and other traditional cardiovascular risk factors²¹.

The finding that loss of *CDKN2B* leads to an increase in the production of *TGFβ1* is interesting, given that *TGFβ1* is generally considered to be a pro-angiogenic cytokine^{22, 23}. However, it is important to note that this concept is based largely on embryonic development data, and that very few studies have examined the effect of post-natal *TGFβ1* modulation in vascular disease models²⁴. Further, it is now appreciated that *TGFβ1* is a complex factor that induces cell- and context-specific effects, including a variety of seemingly antagonistic cellular phenotypes^{25, 26}. For example, *TGFβ1* has well-described 'bifunctional' and dose-dependent properties in the endothelium^{27, 28}. In these cells, *TGFβ1* can either promote migration and tube formation (if *ALK1* and *SMAD 1/5* signaling is triggered), or inhibit angiogenesis (if *ALK5* and *SMAD 2/3* signaling is triggered)^{24, 28}. *TGFβ1* also has protean effects in the SMC, and has separately been reported to promote differentiation (via *CARγ/SRF* interactions)²⁸, inhibit growth (via p38)²⁴, stimulate proliferation (via *PDGF-AA*)²⁸, suppress apoptosis²⁶, inhibit chemokinesis (independent of *SMAD3*)²⁴, or induce extracellular matrix synthesis (including collagen)²⁹, depending on the condition.

One candidate that may partially specify the diverging vascular effects of *TGFβ1* is *TGFβ1i1*. *TGFβ1i1* is a focal adhesion molecule that is induced by *TGFβ1*, and is known to regulate a wide variety of processes including tumorigenesis, cellular senescence, ECM sensing, *TGFβ* auto-induction, and nuclear receptor signaling^{30, 31}. In the vasculature, *TGFβ1i1* appears to play a similarly complicated role, and has been reported to have antagonistic effects on the endothelium and SMC³², as observed in the current study (Figure 3). For example, published gain- and loss-of-function studies suggest that *TGFβ1i1* enhances EC spreading and tube formation in Matrigel^{32, 33}, but inhibits SMC proliferation and migration via myocardin-dependent differentiation^{34, 35}. Indeed, *TGFβ1i1* appears to serve as a *TGFβ* 'rheostat', given its ability to either promote (via *SMAD3*)³⁶ or inhibit (via *SMAD7*)³⁰ downstream signaling. Wang et al. have proposed that the balance of these competing effects may determine whether *TGFβ1* functions as a tumor suppressor or oncogene³⁰, and by extension, whether it promotes or inhibits cell-cycling and angiogenesis.

An important finding in this report is that the observed angiogenic defect is not restricted to hypoxic skeletal muscle, but instead also occurs within human atherosclerotic plaque. This is a significant observation, given that the thin-walled and permeable neovessel has now been associated with leukocyte infiltration and erythrocyte extravasation, and ultimately with atherosclerotic lesion expansion over time^{13, 37}. Our current eQTL findings suggest that carriers of the 9p21 risk allele may experience *TGFβ1* upregulation in the arterial wall *in vivo* (Figure 4C–D), and develop vascular lesions with a disproportionately high number of endothelial tubes that are not stabilized by mural cells (Figure 1), irrespective of plaque size, composition or medical comorbidity (Supplemental Figure I and Table I). Future histopathology studies should investigate whether such individuals are prone to rupture of these immature neovessels, and if intraplaque hemorrhage is a contributor to the robust link between 9p21 risk allele status and coronary artery disease burden.

While we have focused on *CDKN2B* in the current study, it is important to note that debate persists over which gene (or genes) is responsible for the risk encoded by the 9p21 locus. We and others have previously reported that carriers of the risk allele have reduced expression of *CDKN2B* *in vivo*, in circulating cells and cardiovascular tissue^{2, 3, 5, 38, 39}. However, other eQTL studies have reported alternative patterns, and recent work has increasingly associated risk variants with altered expression of a long noncoding RNA known as *ANRIL (CDKN2B-AS1)*⁴⁰⁻⁴². While studies are ongoing to determine whether this candidate gene may also have a direct effect on vascular tissue in humans, *ANRIL* is known to epigenetically suppress the *CDKN2B* promoter⁴³, suggesting that this may be one mechanism by which it could potentiate disease⁴².

A theme which has clearly emerged from the field of 9p21-related research, however, is that genetic variation at this locus appears to alter the behavior of the vascular SMC, and may do so in a context- and disease- specific manner. For example, we have reported that loss of *Cdkn2b* can induce SMC apoptosis in response to an acute injury⁴ or separately render a SMC resistant to efferocytic clearance under conditions of chronic inflammation⁵. Others have studied animals deficient in the entire 9p21 murine ortholog (which display consistent reductions in *Cdkn2b*, but inconsistent changes in *Cdkn2a*), and found that these mice display altered SMC proliferation and senescence at baseline⁴⁴, and a predisposition towards medial degeneration when infused with angiotensin II^{41, 45}. It may be that context-dependent regulation of *TGF β* signaling explains the diverging phenotypes observed. For example, we observed a reduction in upstream *SMAD7* expression under hypoxic conditions in the current study, while Loinard et al. reported an imbalance in canonical downstream *SMAD2* signaling in the SMCs of their aneurysm model⁴⁵. These subtle differences in *TGF β* signaling – which can have major effects on SMC behavior *in vivo*^{24, 28} - could help explain how the 9p21 locus has been simultaneously associated with so many divergent clinical conditions, including non-atherosclerotic intracranial berry aneurysms and atherosclerotic plaque accumulation⁶.

In conclusion, loss of the PAD candidate gene, *Cdkn2b*, appears to impair the ability of the hypoxic neovessel to mature into an oxygen carrying artery, independent of its described effects on plaque accumulation. This process occurs through a novel pathway that involves ‘fine-tuning’ of the *TGF β* pathway, and importantly appears to be reversible, at least in vitro (Figure 5). Given the growing worldwide burden of PAD¹⁰, and the potential relevance of these findings to atherosclerosis in general, these data may inform future translational studies for vascular disease patients.

Supplementary Material

Refer to Web version on PubMed Central for supplementary material.

ACKNOWLEDGEMENTS

We would like to acknowledge Lila Adams for her assistance with the immunohistochemical staining and Tom Quertermous for his mentorship and guidance.

SOURCES OF FUNDING

This study was supported by the National Institutes of Health (1R01HL12522401 and 1R01HL12337001 to NJL; and 1T32HL098049 to KPD) and the American Heart Association (15POST21310005 to VN). The BiKE project was supported by funds from the Swedish Heart and Lung Foundation, the Swedish Research Council (K2009-65X-2233-01-3, K2013-65X-06816-30-4 and 349-2007-8703), Uppdrag Besegra Stroke Study (P581/2011-123), the Strategic Cardiovascular Programs of Karolinska Institutet and Stockholm County Council, and the Stockholm County Council (ALF2011-0260 and ALF-2011-0279).

Nonstandard Abbreviations and Acronyms

CDKN2B	Cyclin-dependent kinase inhibitor 2B
TGFβ1	Transforming growth factor beta 1
PAD	Peripheral Artery Disease
SMC	Smooth muscle cell
EC	Endothelial cell
GWAS	Genome wide association study
TGFβ1i1	Transforming growth factor beta 1 induced 1
ACTA2	Smooth muscle alpha actin
HCASMC	Human coronary artery smooth muscle cells
HUVEC	Human umbilical vein endothelial cells
SmBm	Smooth muscle cell basal medium
EBM-2	Endothelial cell basal-medium-2
siRNA	Small interfering RNA

REFERENCES

- Krimpenfort P, Ijpenberg A, Song JY, van der Valk M, Nawijn M, Zevenhoven J, Berns A. P15ink4b is a critical tumour suppressor in the absence of p16ink4a. *Nature*. 2007; 448:943–946. [PubMed: 17713536]
- Pilbrow AP, Folkersen L, Pearson JF, Brown CM, McNoe L, Wang NM, Sweet WE, Tang WH, Black MA, Troughton RW, Richards AM, Franco-Cereceda A, Gabrielsen A, Eriksson P, Moravec CS, Cameron VA. The chromosome 9p21.3 coronary heart disease risk allele is associated with altered gene expression in normal heart and vascular tissues. *PLoS One*. 2012; 7:e39574. [PubMed: 22768093]
- Motterle A, Pu X, Wood H, Xiao Q, Gor S, Liang Ng F, Chan K, Cross F, Shohreh B, Poston RN, Tucker AT, Caulfield MJ, Ye S. Functional analyses of coronary artery disease associated variation on chromosome 9p21 in vascular smooth muscle cells. *Hum Mol Genet*. 2012
- Leeper NJ, Raiesdana A, Kojima Y, Kundu RK, Cheng H, Maegdefessel L, Toh R, Ahn GO, Ali ZA, Anderson DR, Miller CL, Roberts SC, Spin JM, de Almeida PE, Wu JC, Xu B, Cheng K, Quertermous M, Kundu S, Kortekaas KE, Berzin E, Downing KP, Dalman RL, Tsao PS, Schadt EE, Owens GK, Quertermous T. Loss of cdkn2b promotes p53-dependent smooth muscle cell apoptosis and aneurysm formation. *Arterioscler Thromb Vasc Biol*. 2013; 33:e1–e10. [PubMed: 23162013]
- Kojima Y, Downing K, Kundu R, Miller C, Dewey F, Lancero H, Raaz U, Perisic L, Hedin U, Schadt E, Maegdefessel L, Quertermous T, Leeper NJ. Cyclin-dependent kinase inhibitor 2b regulates efferocytosis and atherosclerosis. *J Clin Invest*. 2014; 124:1083–1097. [PubMed: 24531546]

6. Helgadóttir A, Thorleifsson G, Magnusson KP, Gretarsdóttir S, Steinthorsdóttir V, Manolescu A, Jones GT, Rinkel GJ, Blankensteijn JD, Ronkainen A, Jaaskelainen JE, Kyo Y, Lenk GM, Sakalihan N, Kostulas K, Gottsater A, Flex A, Stefansson H, Hansen T, Andersen G, Weinsheimer S, Borch-Johnsen K, Jorgensen T, Shah SH, Quyyumi AA, Granger CB, Reilly MP, Austin H, Levey AI, Vaccarino V, Palsdóttir E, Walters GB, Jonsdóttir T, Snorraddóttir S, Magnúsdóttir D, Gudmundsson G, Ferrell RE, Sveinbjornsdóttir S, Hernesniemi J, Niemela M, Limet R, Andersen K, Sigurdsson G, Benediktsson R, Verhoeven EL, Tejjink JA, Grobbee DE, Rader DJ, Collier DA, Pedersen O, Pola R, Hillert J, Lindblad B, Valdimarsson EM, Magnadóttir HB, Wijmenga C, Tromp G, Baas AF, Ruigrok YM, van Rij AM, Kuivaniemi H, Powell JT, Matthiasson SE, Gulcher JR, Thorgeirsson G, Kong A, Thorsteinsdóttir U, Stefansson K. The same sequence variant on 9p21 associates with myocardial infarction, abdominal aortic aneurysm and intracranial aneurysm. *Nat Genet.* 2008; 40:217–224. [PubMed: 18176561]
7. Murabito JM, White CC, Kavousi M, Sun YV, Feitosa MF, Nambi V, Lamina C, Schillert A, Coassin S, Bis JC, Broer L, Crawford DC, Franceschini N, Frikke-Schmidt R, Haun M, Holewijn S, Huffman JE, Hwang SJ, Kiechl S, Kollerits B, Montasser ME, Nolte IM, Rudock ME, Senft A, Teumer A, van der Harst P, Vitart V, Waite LL, Wood AR, Wassel CL, Absher DM, Allison MA, Amin N, Arnold A, Asselbergs FW, Aulchenko Y, Bandinelli S, Barbalic M, Boban M, Brown-Gentry K, Couper DJ, Criqui MH, Dehghan A, den Heijer M, Dieplinger B, Ding J, Dorr M, Espinola-Klein C, Felix SB, Ferrucci L, Folsom AR, Fraedrich G, Gibson Q, Goodloe R, Gunjaca G, Haltmayer M, Heiss G, Hofman A, Kieback A, Kiemeny LA, Kolcic I, Kullo IJ, Kritchevsky SB, Lackner KJ, Li X, Lieb W, Lohman K, Meisinger C, Melzer D, Mohler ER 3rd, Mudnic I, Mueller T, Navis G, Oberhollenzer F, Olin JW, O'Connell J, O'Donnell CJ, Palmas W, Penninx BW, Petersmann A, Polasek O, Psaty BM, Rantner B, Rice K, Rivadeneira F, Rotter JI, Seldenrijk A, Stadler M, Summerer M, Tanaka T, Tybjaerg-Hansen A, Uitterlinden AG, van Gilst WH, Vermeulen SH, Wild SH, Wild PS, Willeit J, Zeller T, Zemanek T, Zgaga L, Assimes TL, Blankenberg S, Boerwinkle E, Campbell H, Cooke JP, de Graaf J, Herrington D, Kardina SL, Mitchell BD, Murray A, Munzel T, Newman AB, Oostra BA, Rudan I, Shuldiner AR, Snieder H, van Duijn CM, Volker U, Wright AF, Wichmann HE, Wilson JF, Witteman JC, Liu Y, Hayward C, Borecki IB, Ziegler A, North KE, Cupples LA, Kronenberg F. Association between chromosome 9p21 variants and the ankle-brachial index identified by a meta-analysis of 21 genome-wide association studies. *Circ Cardiovasc Genet.* 2012; 5:100–112. [PubMed: 22199011]
8. Cluett C, McDermott MM, Guralnik J, Ferrucci L, Bandinelli S, Miljkovic I, Zmuda JM, Li R, Tranah G, Harris T, Rice N, Henley W, Frayling TM, Murray A, Melzer D. The 9p21 myocardial infarction risk allele increases risk of peripheral artery disease in older people. *Circ Cardiovasc Genet.* 2009; 2:347–353. [PubMed: 20031606]
9. Downing KP, Nead KT, Kojima Y, Assimes T, Maegdefessel L, Quertermous T, Cooke JP, Leeper NJ. The combination of 9p21.3 genotype and biomarker profile improves a peripheral artery disease risk prediction model. *Vasc Med.* 2014; 19:3–8. [PubMed: 24323119]
10. Fowkes FG, Rudan D, Rudan I, Aboyans V, Denenberg JO, McDermott MM, Norman PE, Sampson UK, Williams LJ, Mensah GA, Criqui MH. Comparison of global estimates of prevalence and risk factors for peripheral artery disease in 2000 and 2010: A systematic review and analysis. *Lancet.* 2013; 382:1329–1340. [PubMed: 23915883]
11. Mahoney EM, Wang K, Cohen DJ, Hirsch AT, Alberts MJ, Eagle K, Mosse F, Jackson JD, Steg PG, Bhatt DL. One-year costs in patients with a history of or at risk for atherosclerosis in the united states. *Circ Cardiovasc Qual Outcomes.* 2008; 1:38–45. [PubMed: 20031786]
12. Kullo IJ, Leeper NJ. The genetic basis of peripheral arterial disease: Current knowledge, challenges, and future directions. *Circ Res.* 2015; 116:1551–1560. [PubMed: 25908728]
13. Sluimer JC, Kolodgie FD, Bijnens AP, Maxfield K, Pacheco E, Kutys B, Duimel H, Frederik PM, van Hinsbergh VW, Virmani R, Daemen MJ. Thin-walled microvessels in human coronary atherosclerotic plaques show incomplete endothelial junctions relevance of compromised structural integrity for intraplaque microvascular leakage. *J Am Coll Cardiol.* 2009; 53:1517–1527. [PubMed: 19389562]
14. Perisic L, Hedin E, Razuvaev A, Lengquist M, Osterholm C, Folkersen L, Gillgren P, Paulsson-Berne G, Ponten F, Odeberg J, Hedin U. Profiling of atherosclerotic lesions by gene and tissue microarrays reveals pcsk6 as a novel protease in unstable carotid atherosclerosis. *Arterioscler Thromb Vasc Biol.* 2013; 33:2432–2443. [PubMed: 23908247]

15. Ahn GO, Seita J, Hong BJ, Kim YE, Bok S, Lee CJ, Kim KS, Lee JC, Leeper NJ, Cooke JP, Kim HJ, Kim IH, Weissman IL, Brown JM. Transcriptional activation of hypoxia-inducible factor-1 (hif-1) in myeloid cells promotes angiogenesis through vegf and s100a8. *Proc Natl Acad Sci U S A*. 2014; 111:2698–2703. [PubMed: 24497508]
16. Niiyama H, Huang NF, Rollins MD, Cooke JP. Murine model of hindlimb ischemia. *J Vis Exp*. 2009
17. Leeper NJ, Tedesco MM, Kojima Y, Schultz GM, Kundu RK, Ashley EA, Tsao PS, Dalman RL, Quertermous T. Apelin prevents aortic aneurysm formation by inhibiting macrophage inflammation. *Am J Physiol Heart Circ Physiol*. 2009; 296:H1329–H1335. [PubMed: 19304942]
18. Leeper NJ, Raiesdana A, Kojima Y, Chun HJ, Azuma J, Maegdefessel L, Kundu RK, Quertermous T, Tsao PS, Spin JM. MicroRNA-26a is a novel regulator of vascular smooth muscle cell function. *J Cell Physiol*. 2011; 226:1035–1043. [PubMed: 20857419]
19. Tusher VG, Tibshirani R, Chu G. Significance analysis of microarrays applied to the ionizing radiation response. *Proc Natl Acad Sci U S A*. 2001; 98:5116–5121. [PubMed: 11309499]
20. Huang da W, Sherman BT, Lempicki RA. Systematic and integrative analysis of large gene lists using david bioinformatics resources. *Nat Protoc*. 2009; 4:44–57. [PubMed: 19131956]
21. Cunnington MS, Keavney B. Genetic mechanisms mediating atherosclerosis susceptibility at the chromosome 9p21 locus. *Curr Atheroscler Rep*. 2011; 13:193–201. [PubMed: 21487702]
22. van Royen N, Hoefler I, Buschmann I, Heil M, Kostin S, Deindl E, Vogel S, Korff T, Augustin H, Bode C, Piek JJ, Schaper W. Exogenous application of transforming growth factor beta 1 stimulates arteriogenesis in the peripheral circulation. *FASEB J*. 2002; 16:432–434. [PubMed: 11821255]
23. Bertolino P, Deckers M, Lebrin F, ten Dijke P. Transforming growth factor-beta signal transduction in angiogenesis and vascular disorders. *Chest*. 2005; 128:585S–590S. [PubMed: 16373850]
24. Goumans MJ, Liu Z, ten Dijke P. Tgf-beta signaling in vascular biology and dysfunction. *Cell Res*. 2009; 19:116–127. [PubMed: 19114994]
25. Gaengel K, Genove G, Armulik A, Betsholtz C. Endothelial-mural cell signaling in vascular development and angiogenesis. *Arterioscler Thromb Vasc Biol*. 2009; 29:630–638. [PubMed: 19164813]
26. Pollman MJ, Naumovski L, Gibbons GH. Vascular cell apoptosis: Cell type-specific modulation by transforming growth factor-beta1 in endothelial cells versus smooth muscle cells. *Circulation*. 1999; 99:2019–2026. [PubMed: 10209007]
27. Carmeliet P. Angiogenesis in health and disease. *Nat Med*. 2003; 9:653–660. [PubMed: 12778163]
28. Bobik A. Transforming growth factor-betas and vascular disorders. *Arterioscler Thromb Vasc Biol*. 2006; 26:1712–1720. [PubMed: 16675726]
29. Kobayashi K, Yokote K, Fujimoto M, Yamashita K, Sakamoto A, Kitahara M, Kawamura H, Maezawa Y, Asaumi S, Tokuhisa T, Mori S, Saito Y. Targeted disruption of tgf-beta-smad3 signaling leads to enhanced neointimal hyperplasia with diminished matrix deposition in response to vascular injury. *Circ Res*. 2005; 96:904–912. [PubMed: 15790953]
30. Wang H, Song K, Krebs TL, Yang J, Danielpour D. Smad7 is inactivated through a direct physical interaction with the lim protein hic-5/ara55. *Oncogene*. 2008; 27:6791–6805. [PubMed: 18762808]
31. Kim-Kaneyama JR, Lei XF, Arita S, Miyauchi A, Miyazaki T, Miyazaki A. Hydrogen peroxide-inducible clone 5 (hic-5) as a potential therapeutic target for vascular and other disorders. *J Atheroscler Thromb*. 2012; 19:601–607. [PubMed: 22472216]
32. Komorowsky C, Samarin J, Rehm M, Guidolin D, Goppelt-Struebe M. Hic-5 as a regulator of endothelial cell morphology and connective tissue growth factor gene expression. *J Mol Med (Berl)*. 2010; 88:623–631. [PubMed: 20333347]
33. Avraamides C, Bromberg ME, Gaughan JP, Thomas SM, Tsygankov AY, Panetti TS. Hic-5 promotes endothelial cell migration to lysophosphatidic acid. *Am J Physiol Heart Circ Physiol*. 2007; 293:H193–H203. [PubMed: 17337598]
34. Wang X, Hu G, Betts C, Harmon EY, Keller RS, Van De Water L, Zhou J. Transforming growth factor-beta1-induced transcript 1 protein, a novel marker for smooth muscle contractile phenotype,

- is regulated by serum response factor/myocardin protein. *J Biol Chem.* 2011; 286:41589–41599. [PubMed: 21984848]
35. Kim-Kaneyama JR, Wachi N, Sata M, Enomoto S, Fukabori K, Koh K, Shibamura M, Nose K. Hic-5, an adaptor protein expressed in vascular smooth muscle cells, modulates the arterial response to injury in vivo. *Biochem Biophys Res Commun.* 2008; 376:682–687. [PubMed: 18812162]
 36. Wang H, Song K, Sponseller TL, Danielpour D. Novel function of androgen receptor-associated protein 55/hic-5 as a negative regulator of smad3 signaling. *J Biol Chem.* 2005; 280:5154–5162. [PubMed: 15561701]
 37. Michel JB, Virmani R, Arbustini E, Pasterkamp G. Intraplaque haemorrhages as the trigger of plaque vulnerability. *Eur Heart J.* 2011; 32:1977–1985. 1985a, 1985b, 1985c. [PubMed: 21398643]
 38. Liu Y, Sanoff HK, Cho H, Burd CE, Torrice C, Mohlke KL, Ibrahim JG, Thomas NE, Sharpless NE. Ink4/arf transcript expression is associated with chromosome 9p21 variants linked to atherosclerosis. *PLoS ONE.* 2009; 4:e5027. [PubMed: 19343170]
 39. Svensson PA, Wahlstrand B, Olsson M, Froguel P, Falchi M, Bergman RN, McTernan PG, Hedner T, Carlsson LM, Jacobson P. Cdkn2b expression and subcutaneous adipose tissue expandability: Possible influence of the 9p21 atherosclerosis locus. *Biochem Biophys Res Commun.* 2014; 446:1126–1131. [PubMed: 24680834]
 40. Holdt LM, Beutner F, Scholz M, Gielen S, Gabel G, Bergert H, Schuler G, Thiery J, Teupser D. Anril expression is associated with atherosclerosis risk at chromosome 9p21. *Arterioscler Thromb Vasc Biol.* 2010; 30:620–627. [PubMed: 20056914]
 41. Cunnington MS, Santibanez Koref M, Mayosi BM, Burn J, Keavney B. Chromosome 9p21 snps associated with multiple disease phenotypes correlate with anril expression. *PLoS Genet.* 2010; 6:e1000899. [PubMed: 20386740]
 42. Johnson AD, Hwang SJ, Voorman A, Morrison A, Peloso GM, Hsu YH, Thanassoulis G, Newton-Cheh C, Rogers IS, Hoffmann U, Freedman JE, Fox CS, Psaty BM, Boerwinkle E, Cupples LA, O'Donnell CJ. Resequencing and clinical associations of the 9p21.3 region: A comprehensive investigation in the framingham heart study. *Circulation.* 2013; 127:799–810. [PubMed: 23315372]
 43. Yu W, Gius D, Onyango P, Muldoon-Jacobs K, Karp J, Feinberg AP, Cui H. Epigenetic silencing of tumour suppressor gene p15 by its antisense rna. *Nature.* 2008; 451:202–206. [PubMed: 18185590]
 44. Visel A, Zhu Y, May D, Afzal V, Gong E, Attanasio C, Blow MJ, Cohen JC, Rubin EM, Pennacchio LA. Targeted deletion of the 9p21 non-coding coronary artery disease risk interval in mice. *Nature.* 2010; 464:409–412. [PubMed: 20173736]
 45. Loinard C, Basatemur G, Masters L, Baker L, Harrison J, Figg N, Vilar J, Sage AP, Mallat Z. Deletion of chromosome 9p21 noncoding cardiovascular risk interval in mice alters smad2 signaling and promotes vascular aneurysm. *Circ Cardiovasc Genet.* 2014; 7:799–805. [PubMed: 25176937]

Novelty and Significance

What Is Known?

- Genome-wide association studies (GWAS) have unequivocally identified loci associated with cardiovascular disease.
- The mechanism by which the top GWAS locus promotes disease remains unknown.

What New Information Does This Article Contribute?

- Subjects who carry the top cardiovascular GWAS risk allele harbor atherosclerotic lesions with a high burden of immature intraplaque vessels.
- Mice deficient in a related candidate gene display a vascular maturation defect, even under non-atherosclerotic conditions.
- Genetic variation may promote cardiovascular disease not only by promoting plaque growth, but also by impairing vascular maturation.

Peripheral artery disease (PAD) results from defects in atherogenesis and angiogenesis. Genomic variants at the chromosome 9p21 cardiovascular GWAS locus have been associated with the heritable risk for both coronary artery disease (CAD) and PAD. *CDKN2B* is a 9p21 candidate gene which has previously been shown to regulate atherogenesis. Whether this gene also regulates angiogenesis is unknown. The current study reveals that the 9p21 risk allele is correlated with microvessel density within the atherosclerotic plaque, independent of lesion size or medical comorbidity. Mice deficient in *Cdkn2b* develop advanced hindlimb ischemia due to a defect in the maturation of immature blood vessels, even under non-atherosclerotic conditions. Signaling studies indicate that this phenomenon occurs due to a previously unrecognized defect in *TGF β* -dependent SMC-recruitment to the nascent blood vessel. This work may inform future translational studies aimed at: 1. Promoting the development of oxygen-carrying blood vessels for patients with PAD; or 2. Stabilizing rupture-prone intraplaque neovessels for patients with CAD.

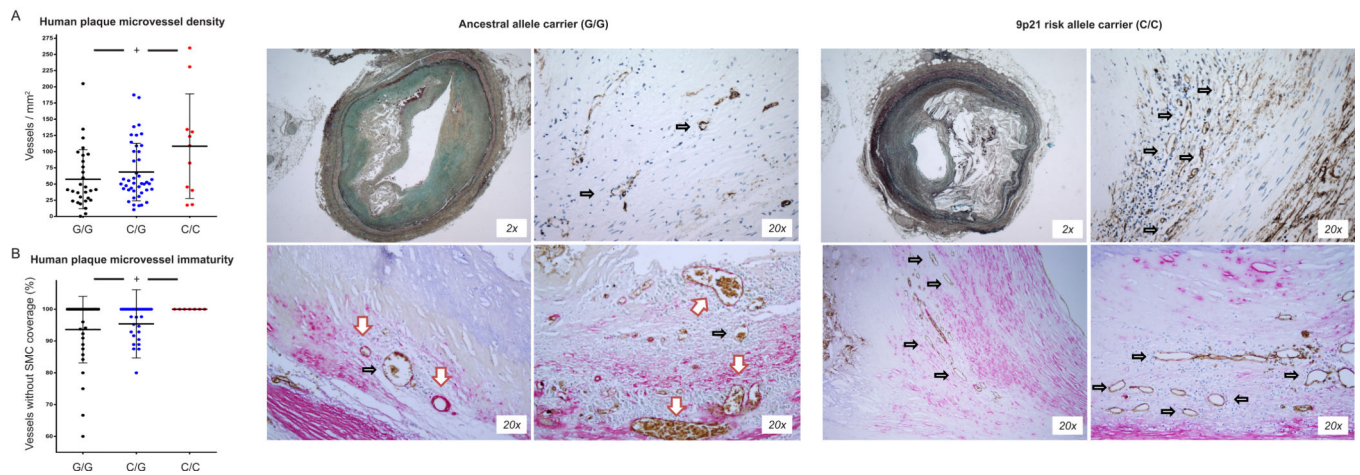


Figure 1. Carriers of the 9p21 risk allele display pathological neoangiogenesis within their atherosclerotic plaques

A. Quantitative morphometric analysis revealed that carriers of the representative 9p21 risk allele ('C' at rs1333049 in red) have a significantly higher burden of intraplaque microvessels than carriers of the ancestral allele ('G' in black, P for trend = 0.02, representative images of Movat pentachrome on left (2 \times) and CD31/CD34 endothelial cells on right (20 \times)) Black arrows indicate endothelial tubes. **B.** Immunohistochemistry revealed that mural cell coverage of the lesional neovessel is significantly reduced amongst carriers of the 9p21 risk allele, such that 100% of these immature vessels do not become enveloped by adjacent SMCs (P for trend < 0.05). Representative images shown at right for each (Ulex(brown)/ α SMA(red) double staining (20 \times)) Red arrows represent endothelial tubes surrounded by SMCs, black arrows represent vessels not surrounded by SMCs.

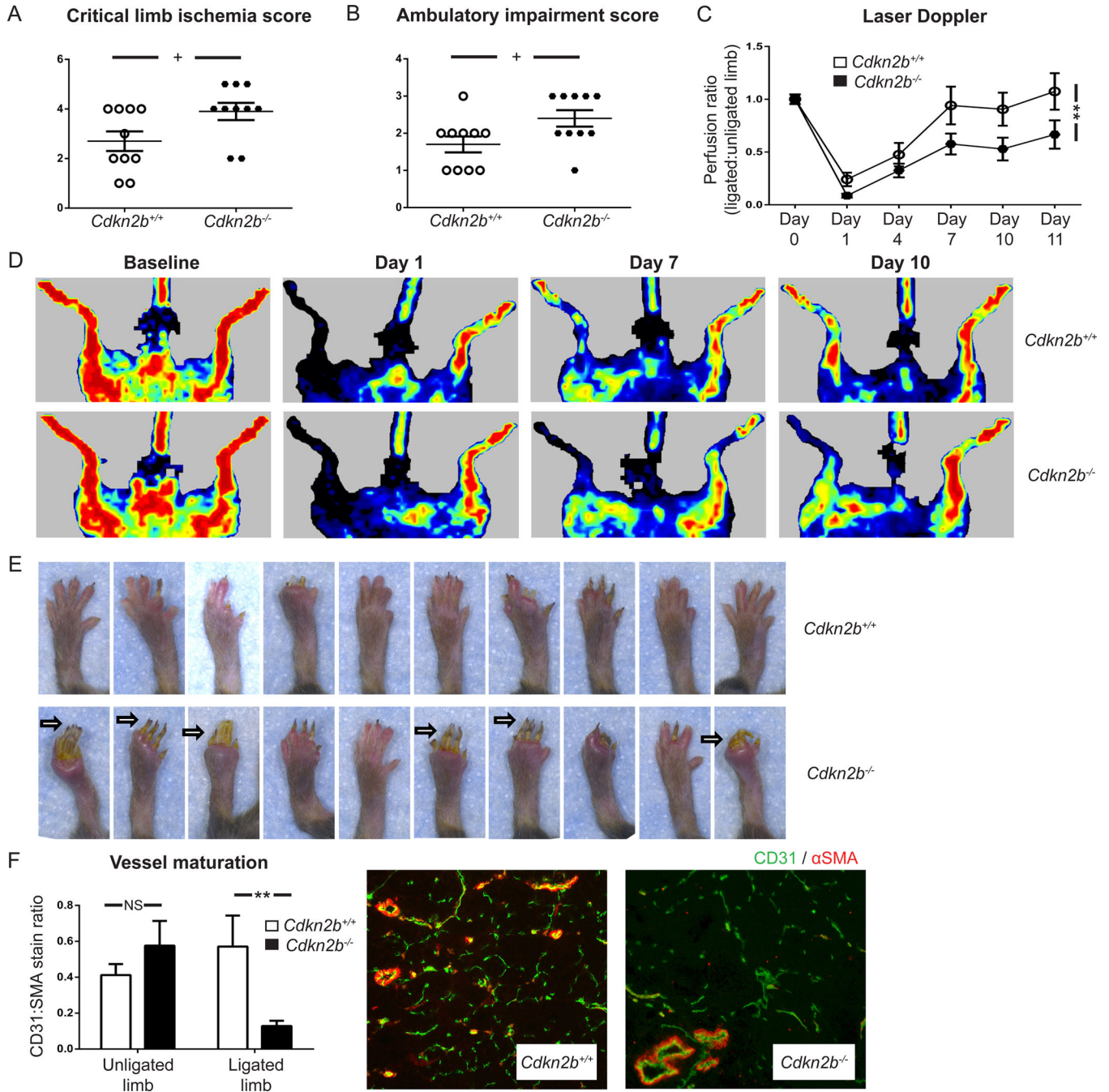


Figure 2. Loss of *Cdkn2b* impairs neovessel maturation and promotes hindlimb ischemia in a non-atherosclerotic model of peripheral artery disease
 Compared to wild type mice, *Cdkn2b*^{-/-} mice developed advanced hindlimb ischemia after femoral artery ligation, as quantified by blinded critical limb ischemia scoring (A) and ambulatory impairment assessment (B, $P < 0.05$ for each). C. Laser Doppler imaging confirmed that the hindlimb ischemia phenotype was secondary to a perfusion defect observable as soon as 7 days after femoral artery ligation ($P < 0.0001$ via two way ANOVA; representative images shown in (D)). E. Representative images reveal that *Cdkn2b*^{-/-} mice sustain a disproportionate amount of tissue loss and digital autoamputation (arrows), relative

to *Cdkn2b*^{+/+} mice. **F.** Simultaneous immunofluorescence staining revealed that the ratio of SMCs (α -SMA, red) to ECs (CD31, green) is severely reduced in the ischemic hindlimb of *Cdkn2b*^{-/-} mice relative to *Cdkn2b*^{+/+} mice ($P < 0.01$), confirming that a vessel maturation defect occurs under nonatherosclerotic conditions. + < 0.05, # <0.01, ** <0.001

Author Manuscript

Author Manuscript

Author Manuscript

Author Manuscript

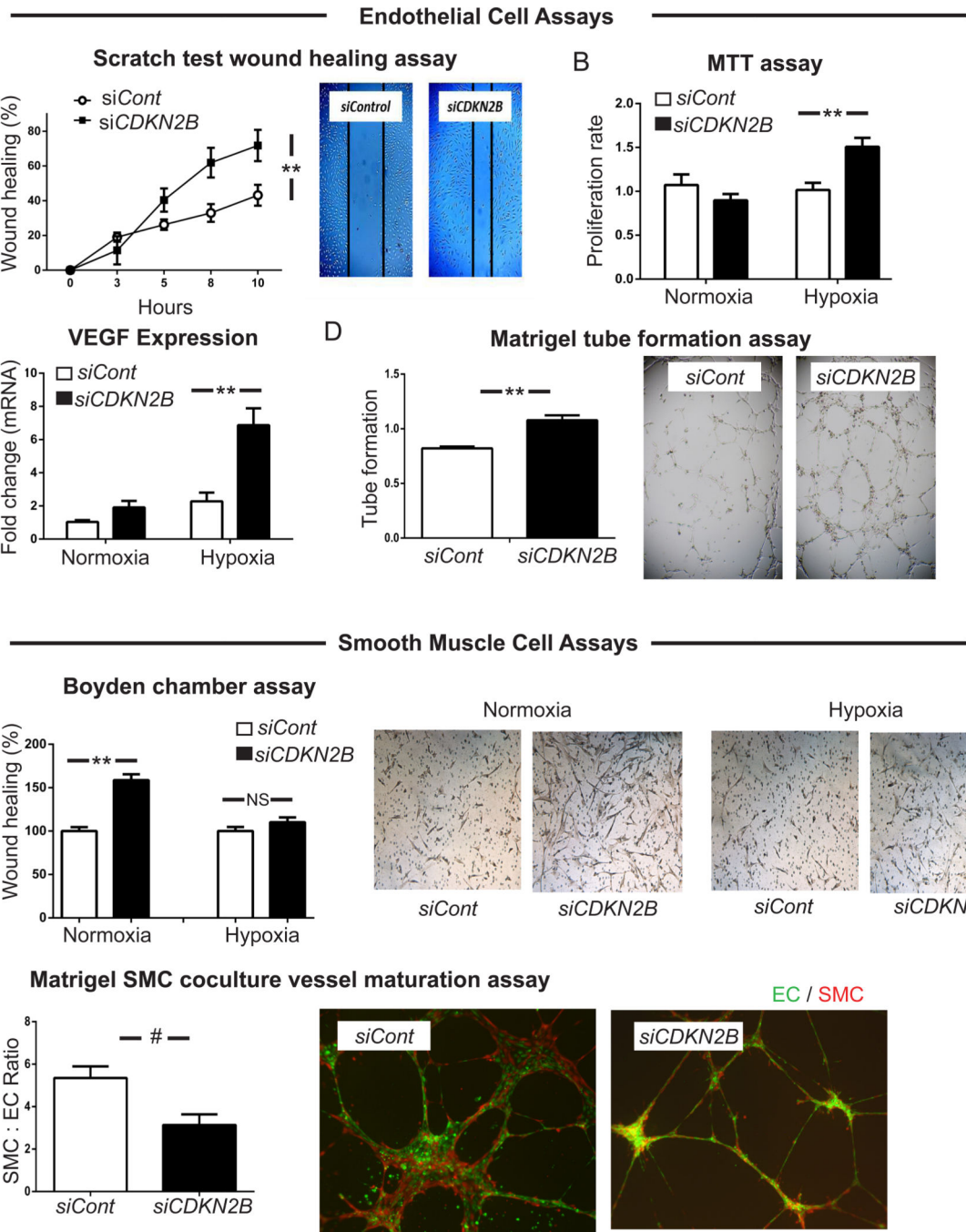


Figure 3. Loss of *CDKN2B* promotes EC angiogenesis, but inhibits SMC recruitment to hypoxic neovessels in vitro

Relative to control-transfected (siCont) cells, hypoxic *CDKN2B*-deficient (siCDKN2B) ECs displayed several pro-angiogenic features including: **A.** Increased ‘wound healing’ in a scratch assay ($P < 0.001$); **B.** Increased proliferation in an MTT assay ($P < 0.001$); **C.** Upregulation of the angiogenic cytokine *VEGF* ($P < 0.001$); and **D.** Increased tube formation in a Matrigel assay ($P < 0.001$). **E.** Conversely, *CDKN2B*-deficient SMCs lose their baseline growth advantage (left, $P < 0.001$) under hypoxic conditions (right, $P = NS$).

F. This defect correlates with an inability of *CDKN2B*-deficient endothelial tubes to mature into vessels covered by mural cells, when co-cultured with *CDKN2B*-deficient SMCs ($P < 0.05$ relative to assay performed with siCont ECs and SMCs). + < 0.05 , # < 0.01 , ** < 0.001

Author Manuscript

Author Manuscript

Author Manuscript

Author Manuscript

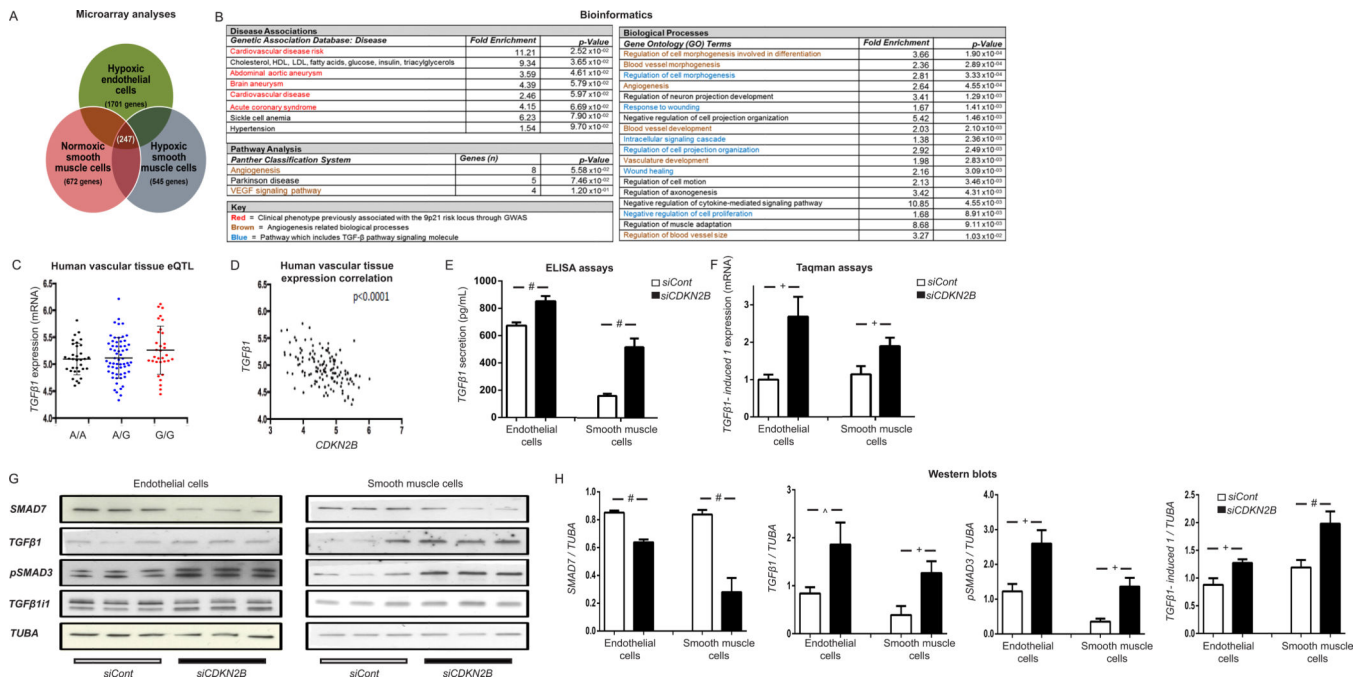


Figure 4. Loss of *CDKN2B* leads to impaired *TGFβ* signaling

A. Genome-wide cDNA microarrays performed in *CDKN2B*-deficient ECs and SMCs revealed a list of 247 genes which were consistently dysregulated under each condition tested, relative to control-transfected cells (>1.5 Fold change, FDR < 1). **B.** Bioinformatic analyses of these differentially regulated genes reveals that loss of *CDKN2B* is predicted to be associated with several cardiovascular phenotypes previously associated with the 9p21 locus through GWAS (red), according to the Genetic Association Database for Disease Associations. DAVID evaluation of overabundant canonical pathways and GO biological processes associated with these genes revealed a clear link to angiogenesis-related phenomena (brown). Of particular note is the significant number of processes which include at least one regulated *TGFβ*-pathway member (blue). **C.** Expression Quantitative Locus (eQTL) analysis of a set of 96 human plaques suggested that carriers of the representative 9p21 risk allele (‘G’ at rs1412829) experience a trend towards increased *TGFβ1* expression within the vessel wall ($P = 0.07$). **D.** Co-expression analysis performed in an overlapping set of $n = 127$ plaques confirmed that *CDKN2B* and *TGFβ1* are anti-correlated in arterial tissue ($P < 0.0001$). **E.** ELISA assays confirmed that knock down of *CDKN2B* leads to increased *TGFβ1* secretion in both hypoxic ECs and SMCs ($P < 0.01$ for each). **F.** Taqman assays confirmed that *TGFβ1i1*, the *TGFβ* effector molecule most consistently altered in the microarrays presented above, is significantly upregulated in hypoxic *CDKN2B*-deficient ECs and SMCs, relative to control-transfected cells ($P < 0.05$ for each). Western blot assays (**G**) and corresponding protein quantification (**H**) aimed at determining the mechanism by which loss of *CDKN2B* perturbs *TGFβ* signaling revealed that loss of *CDKN2B* in ECs and SMCs leads to: 1. Downregulation of the inhibitory factor, *SMAD7*; 2. *TGFβ1* auto-induction; 3. Downstream *SMAD3* phosphorylation; and 4. Upregulation of the vasoactive factor, *TGFβ1i1*. ^ = 0.05, + < 0.05, # < 0.01, ** < 0.001

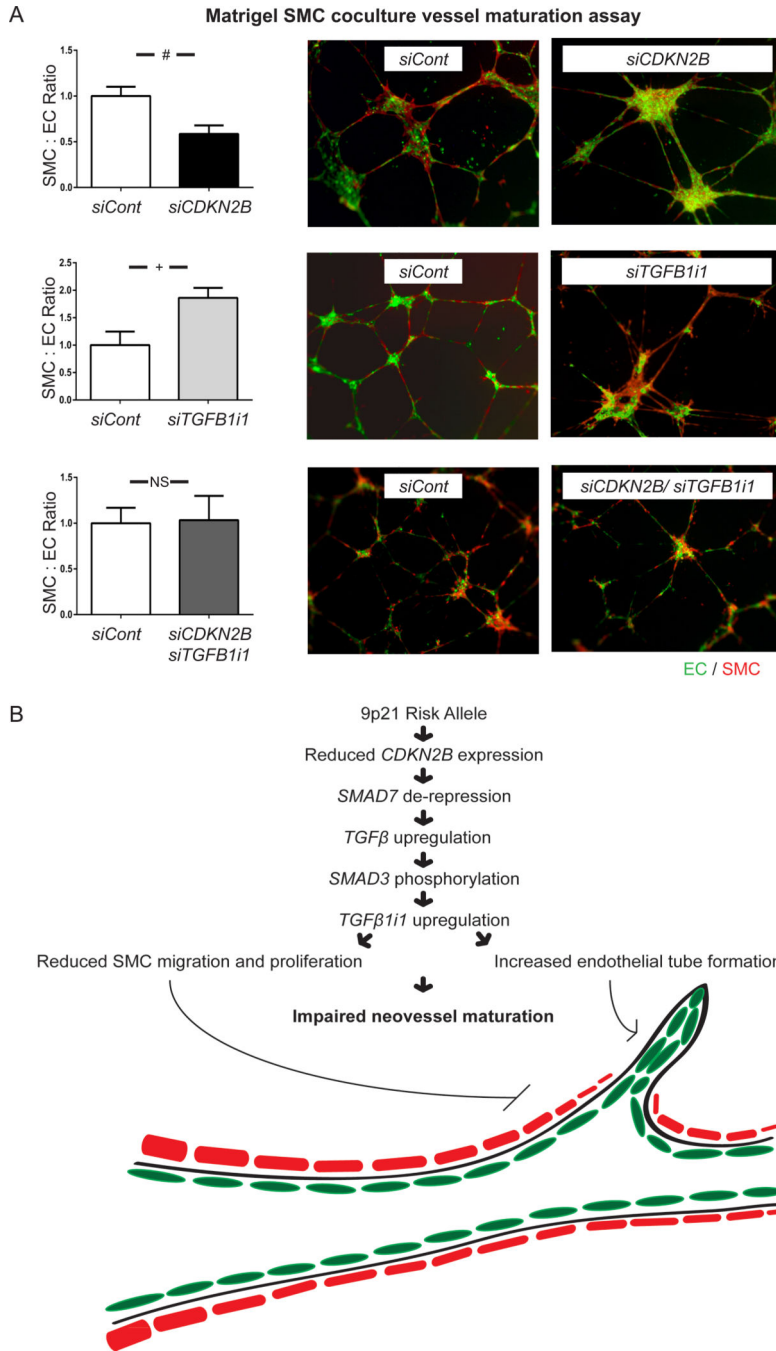


Figure 5. The *CDKN2B*-dependent defect in vessel maturation is reversible, in vitro
A. Compared to the opposing effects observed with individual knockdown of *CDKN2B* (41.4% reduction in vessel maturation, $P < 0.001$) and *TGFβ1i1* (86.1% increase in vascular maturation, $P < 0.02$), simultaneous siRNA knockdown of both *CDKN2B* and *TGFβ1i1* led to a complete normalization of the baseline Matrigel tube maturation defect, indicating that the phenomenon may be reversible, at least in vitro ($P = 0.92$, relative to control transfected

cells). **B.** Proposed molecular signaling mechanism for how *CDKN2B* may mediate its angiogenic effects.

Author Manuscript

Author Manuscript

Author Manuscript

Author Manuscript